Experimental Studies of the Effects of Anode Composition and Process Parameters on Anode Slime Adhesion and Cathode Copper Purity by Performing Copper Electrorefining in a Pilot-Scale Cell

WEIZHI ZENG, SHIJIE WANG, and MICHAEL L. FREE

Copper electrorefining tests were conducted in a pilot-scale cell under commercial tankhouse environment to study the effects of anode compositions, current density, cathode blank width, and flow rate on anode slime behavior and cathode copper purity. Three different types of anodes (high, mid, and low impurity levels) were used in the tests and were analyzed under SEM/EDS. The harvested copper cathodes were weighed and analyzed for impurities concentrations using DC Arc. The adhered slimes and released slimes were collected, weighed, and analyzed for compositions using ICP. It was shown that the lead-to-arsenic ratio in the anodes affects the sintering and coalescence of slime particles. High current density condition can improve anode slime adhesion and cathode purity by intensifying slime particles' coalescence and dissolving part of the particles. Wide cathode blanks can raise the anodic current densities significantly and result in massive release of large slime particle aggregates, which are not likely to contaminate the cathode copper. Low flow rate can cause anode passivation and increase local temperatures in front of the anode, which leads to very intense sintering and coalescence of slime particles. The results and analyses of the tests present potential solutions for industrial copper electrorefining process.

DOI: 10.1007/s11663-016-0736-4

I. INTRODUCTION

ANODES used in copper electrorefining come from smelters and the existence of impurities in copper melt leads to inclusion formation in grain boundaries within copper anodes.[1] Some of these inclusion particles are soluble and the impurities inside are dissolved into electrolyte during electrorefining. However, most of the inclusions are refractory and become anode slimes as copper around them dissolves.[1] These anode slime particles can vary in size and density.[1,2] Large and heavy slimes are difficult to transport in flowing electrolyte and usually settle down, but small slimes can suspend in electrolyte and be entrapped in cathode copper, resulting in cathode contamination.[3–5]

The mineralogy and structures of inclusions and anode slimes have been studied by researchers. According to Chen and Dutrizac's work, the major inclusions and phases in anodes are Kupferglimmer structure, Cu_2O, $Cu_2(Se, Te)$, selenide spheroid, NiO, Group VB elements-enriched compounds.[6–11] They also indicated that the major phases and structures in anode slimes include $(Cu, Ag)_2Se$, Kupferglimmer structure, lead sulfate, Group VB elements-enriched compounds, euhedral NiO crystals.[6,9–15] Besides, the precipitation of dissolved impurities and its effect on cathode purity has also been studied. Precipitates that are amorphous and have compositions of Bi-As-O and Sb-As-O, are referred to as floating slimes and can cause cathode quality deterioration.[16] Crystalline precipitates that are formed by homogeneous precipitation of arsenic, antimony, and bismuth, can be used to remove dissolved impurities from the electrolytic solution.[17,18] Furthermore, the slime adhesion on the anode is significant for impurity control in electrorefining and some studies on it have been done.[2] In addition, flow studies involving slime particles have been performed by both experiments and simulations.[3–5]

In our previous research, the sintering and coalescence of slime particles and its effects on anode slime adhesion and cathode purity were studied.[2] Significant findings can be summarized[2]: the sizes of slime particles can be increased by their sintering/coalescence; anode slime adhesion increases from room temperature to a peak adhesion temperature [the peak adhesion temperatures are around 333.15 K (60 °C) for most anodes] and then decreases as cell temperature goes up further, due to the effects of slime particle sintering/coalescence;

WEIZHI ZENG, Graduate Research Assistant, and MICHAEL L. FREE, Professor and Associate Chair, are with the Department of Metallurgical Engineering, University of Utah, Salt Lake City, UT 84108. Contact e-mail: weizhi.zeng@utah.edu SHIJIE WANG, Principal Advisor, is with Rio Tinto Kennecott Utah Copper, Magna, UT 84044.

Manuscript submitted April 1, 2016.
Article published online June 30, 2016.

slime particles tend to fall off the anode after the peak adhesion temperature because of their larger and larger sizes (these slime particles are generally larger than 9 to 10 μm[2]); slime particles with Pb-Bi-S shells have lower sintering temperatures and are easier to coalesce together and/or adhere to the anode than those with Pb-Bi-S-As shells; anodes having more slime particles with Pb-Bi-S shells demonstrate lower peak adhesion temperatures than anodes having more slime particles with Pb-Bi-S-As shells; better anode slime adhesion and/or larger slime particle sizes lead to cathode copper with higher purity.

Copper users prefer low bismuth levels, as bismuth is an undesirable element in copper cathode. It is likely that the existing 0.5 ppm Bi-targeted limit will be lowered in the future. Therefore, there is a need to lower bismuth levels in cathodes to ensure high productivity of high-quality copper. It is generally observed that high slime adhesion reduces cathode impurities by making the anode slime particles less likely to be transported and deposited in the cathode. Thus the understanding of slime adhesion and transport in copper electrorefining is critical to refineries. Nevertheless, systematic studies of anode composition and process parameters on the adhesion, mobility, and transport of anode slimes can be rarely found in the past research and are worth for further study. Therefore, a series of copper electrorefining tests have been performed, using anodes with different compositions under different experimental conditions, in a pilot-scale electrorefining cell made of transparent walls. By using anodes cut from commercial cell standard anodes, circulating electrolyte from tankhouse pipeline system, and performing the tests in the tankhouse environment, these experimental copper electrorefining tests were designed to be as close to real industrial process as possible. The resulting cathodes, slime particles, and anodes were analyzed, with the fluid flow field in the cell studied by experimental measurement and simulation in other paper.[5] Lead-to-arsenic ratio is proposed in this manuscript to be incorporated in refinery practice to control slime adhesion and transport. It can help refineries to control cathode contamination by providing a view of the process from a different angle. Currently, most copper refineries use As/(Bi + Sb) ratio and/or As/Sb ratio for contamination control as these have been widely studied in the past decades.[19–23] While the impurities concentrations in electrolyte are adjusted according to the As/(Bi + Sb) ratio, the impurities levels in the anodes can also be adjusted according to the Pb/As ratio. Their combination can provide better control of the entire copper electrorefining process and further reduce impurity levels in the cathode including bismuth.

From the results of the impurities levels of harvested cathodes and the compositions and weights of adhered slimes and released slimes, the effects of process parameters and anode compositions on the behavior of slime particles and the purity of cathode copper can be analyzed. From SEM/EDS analysis of inclusions in different anodes, as well as slime particles and cathode copper, the underlying mechanisms are discussed.

II. EXPERIMENTAL

The experiments were performed in the tankhouse of Rio Tinto Kennecott Refinery. A pilot-scale electrorefining cell built with transparent and acid-resistive Lexan and supported by steel tube frames sits on the tankhouse floor is shown in Figure 1. The dimensions of the cell are 50 inches (1.27 m) height × 12 inches (0.30 m) depth × 8.5 inches (0.22 m) width, while the electrolyte domain in the cell has dimensions of 48 inches (1.22 m) height × 10.875 inches (0.28 m) depth × 7 inches (0.18 m) width. A flow dispersion block (7.25 inches (0.18 m) length × 1 inch (0.025 m) depth × 2 inches (0.050 m) height) is located at the side wall 6 inches (0.15 m) above the bottom of the cell, with four circular openings [0.25 inches (0.0064 m) in diameter] distributed on it. A 0.25-inch (0.0064 m) manual valve outside the cell is connected with the flow distributor. An outlet weir about 7 inches (0.18 m) length × 1.25 inches (0.032 m) depth × 2 inches (0.050 m) height is located at the top of the cell, connected with pipes. A 0.5 inches (0.013 m) drain valve is located at the bottom of a side wall opposite to the flow dispersion block. The electrolyte inflow goes through the flow dispersion block and enters the cell through the four circular openings. The baseline flow rate is about 5 mL/sec and is determined by the inflow velocity (0.0488 m/s, same as Kennecott commercial cells) and the total inlet area. At the top of the cell, the electrolyte overflows to the outlet weir and flows into the

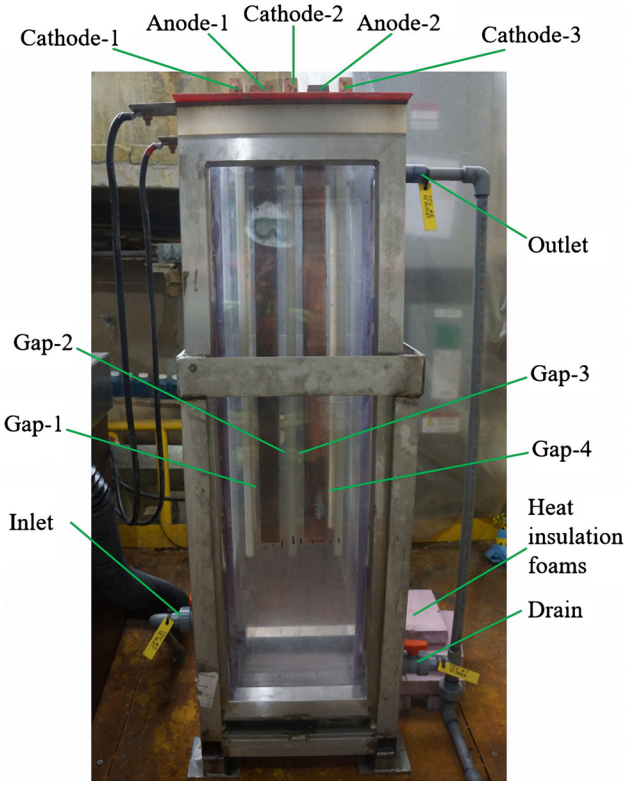

Fig. 1—The pilot-scale copper electrorefining cell used in the experiments with its major components labeled.

connected pipe. The drain valve is closed during the tests and open after each test to collect slimes in the cell. The electrolyte used for the tests comes directly from the tankhouse circulation system and have impurities concentrations shown in Table I.

Electric current is provided by a rectifier, which is connected with two metal plates on the top of the cell. One metal plate sits on the north side wall of the cell and connects to the positive pole of the rectifier, and the other plate is on the south side wall and connected to the negative pole. All copper anodes are in touch with the north metal plate and insulated from the south plate, while all cathode blanks touch the south metal plate and are insulated from the north plate. There are two anodes (shown as A-1 and A-2 in Figure 1) and three cathode blanks (shown as C-1, C-2, and C-3, respectively in Figure 1) symmetrically placed in the cell, with a distance of about 1 inch (0.025 m) between each adjacent anode and cathode and a distance of about 4 inches (0.10 m) between the centers of the two anodes. Each anode is about 4.2 inches (0.11 m) in width, 1.5 inches (0.038 m) in depth, and 35.5 inches (0.90 m) in height (32.25 inches (0.82 m) under electrolyte level). Three different types of anodes were used in the experiments (as shown in Table II) and were analyzed for compositions by DC Arc. The results are shown in Table III. Figure 2 shows the photo of one anode as an example. There are two types of cathode blanks utilized in the tests: the normal cathode blanks and the wide cathode blanks. Each normal cathode blank is 3.5 inches (0.089 m) in width, 0.3 inches (0.0076 m) in depth, and 36.625 inches (0.93 m) in height (33.375 inches (0.85 m) immersed in electrolyte); and each wide cathode blank is 4.75 inches (0.12 m) in width, with the same depth and height dimensions as the normal one. The cathode blanks are made of stainless steel. The total current applied is determined by the applied current density (240 A/m^2 baseline current density) and the total cathodic area. Note that the back sides of Cathode-1 and Cathode-3 are coated with electric insulation paint, in order to have better current density distribution in the cell. The baseline electrolyte temperature is about 334 K (61 °C). The side walls of the cell are covered by heat insulation foams as to maintain constant cell temperature. Each test has two cycles of 11 days. The experimental conditions applied in each test are summarized in Table II.

III. RESULTS

Mostly in terms of lead, arsenic, and bismuth, the type-1 anode has mid-level impurities contents; the type-2 anode has high-level impurities especially for lead; and the type-3 anode has low contents of impurities.

Four strips of deposited copper could be harvested from each test: one from cathode-1, two from cathode-2, and one from cathode-3. A photo of a copper strip on a cathode blank is shown in Figure 3. These copper strips were weighed and analyzed by DC Arc for compositions. The current efficiency for each test and the current density on each cathode can be estimated based on the weights of cathode copper. The results for each test are shown in Tables IV and V. Note that Cathode-2-W and Cathode-2-E represent the copper strips on the west and east sides of Cathode-2, respectively.

From the results shown in Table IV, the current densities on the cathodes vary in a reasonable range around the average value in the tests. This is because that the contact resistance of the connection between the sitting arm of the cathode blank and the metal plate connected to the negative pole is slightly different among

Table I. The Content of the Electrolyte from the Tankhouse Circulation System

Electrolyte Constitute	Cu	H_2SO_4	Bi	Fe	Ni	Pb	Sb	Se
Concentration (g/L)	44.82	168.37	0.04	0.15	2.80	0.01	0.10	<0.001

Table II. Experimental Conditions Applied for Each Copper Electrorefining Test

Condition	Test-1	Test-2	Test-3	Test-4	Test-5	Test-6	Test-7
Anode	type-1	type-2	type-3	type-1	type-1	type-2	type-2
Cathode	normal	normal	normal	normal	wide	wide	wide
Flow rate (mL/s)	5	5	5	5	5	2.5	5
Current density (A/m^2)	240	240	240	300	240	240	240
Temperature (K)	334	334	334	334	334	334	330

Table III. The Compositions of the Anodes Used in the Experiments

Anode Type	Pb	As	Bi	Se	Sb	Ni	Fe	Te	Sn
1	0.198	0.19	0.049	0.067	<0.0023	0.044	<0.0020	0.008	0.001
2	0.505	0.26	0.068	0.051	0.012	0.031	<0.0018	0.012	0.001
3	0.195	0.113	0.036	0.051	0.008	0.021	<0.0019	0.006	0.001

All units in weight percent.

three cathode blanks. Note that minor current is distributed on the coated side of Cathode-1 and Cathode-3 due to some penetration through the paint. The current density on each cathode is calculated based on the following equation according to Faraday's Law:

$$\text{Current\_}D = \frac{nFW}{\beta MAt},$$

where n is the number of electrons transferred, F is Faraday constant, W is the actual weight of the cathode copper, β is the estimated current efficiency, M is the molecular weight for copper, A is the cathodic area, and t is the total time.[24]

The current efficiency for each test is estimated through the equation given below and is above 97 pct for all tests.

Fig. 2—The specially cut copper anode used in the copper electrorefining experiments.

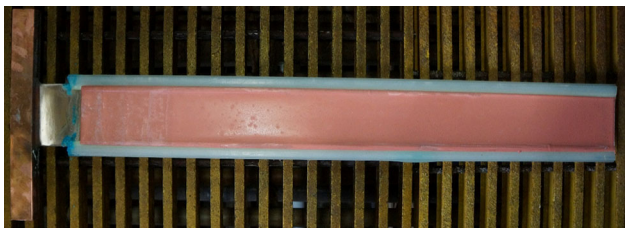

Fig. 3—The unstripped cathode copper on a cathode blank after the copper electrorefining experiment.

$$\text{Current\_Efficiency} = \frac{\text{Actual\_Weight}}{\text{Theoretical\_Weight}} = \frac{W}{\frac{ItM}{nF}} = \frac{nFW}{ItM},$$

where W is the actual weight of the harvested copper, I is the total current applied, and t is the total time of the test.[24]

Table V shows the concentrations of major impurities in the harvested cathode copper. The significant impurities are bismuth, lead, sulfur, selenium, and arsenic, which will be mainly discussed in this paper. The most concerned impurity is bismuth, and the aim of the tests is to reduce bismuth content in cathode copper. Bismuth is one of the most detrimental elements in copper, as it significantly reduces the ductility of copper and affects the production of copper rod and wire. The target bismuth level in the cathode copper is below 0.2 ppm.

As shown in Table II, Test-1 acts as the control experiment, with normal levels of test conditions and the type-1 anodes with mid-level impurities concentrations. Test-2 uses the type-2 anodes with high-level impurities concentrations especially for lead, and the corresponding results show less bismuth levels in the harvested copper in comparison with Test-1. Test-3 uses the type-3 low impurity level anodes and the resulting cathode copper also has low impurities contents except Cathode-3, which was a little tilted to Anode-2 in the test and might therefore get more slime particles entrapped. Test-4 examines the effect of current density on the results as it was conducted at 300 A/m^2. The results show that high current density has the effect of reducing bismuth levels in cathode copper, as compared with Test-1. From Test-5, the wide cathode blanks were utilized for the experiments and the impurities contents in the harvested copper from the wide blanks were well controlled as compared with Test-1. However, some impurity concentration differences between the edge and the center of the cathode copper were observed, which will be discussed in Section IV–C. Test-6 was designed to run at low flow rate (2.5 mL/s) using the type-2 anodes and the wide cathode blanks, and the bismuth

Table IV. Weights, Current Densities, and Current Efficiencies for the Cathodes Harvested in Each Copper Electrorefining Test

	Test-1		Test-2		Test-3		Test-4	
	Weight	Current_D	Weight	Current_D	Weight	Current_D	Weight	Current_D
Cathode-1	5.20	246.26	6.11	253.03	4.67	215.18	5.29	309.98
Cathode-2	9.58	226.64	11.44	236.90	9.76	225.10	10.85	318.21
Cathode-3	4.26	201.47	4.99	206.52	5.80	267.40	4.34	254.20
Current efficiency (percent)	98.87		98.13		97.28		98.97	

	Test-5		Test-6		Test-7	
	Weight	Current_D	Weight	Current_D	Weight	Current_D
Cathode-1	7.13	204.24	6.32	222.70	7.69	272.16
Cathode-2	16.71	239.42	13.00	229.09	11.38	201.32
Cathode-3	9.59	274.74	7.65	269.64	7.79	275.53
Current efficiency (percent)	99.49		98.59		98.55	

Weight in the unit of kg and current density in the unit of A/m^2.

Table V. Impurities Concentrations in the Cathode Copper Harvested from Each Electrorefining Test

Impurity	Bi	Pb	As	Se	Sb	Ni	Fe	Sn	Te
Test 1									
Cathode-1	0.17	<0.500	<1.000	<0.500	<1.00	<1.0	4.3	<0.500	<0.500
Cathode-2-W	0.13	<0.500	<1.000	<0.500	<1.00	<1.0	<3.0	<0.500	<0.500
Cathode-2-E	<0.100	<0.500	1.13	<0.500	<1.00	<1.0	<3.0	<0.500	<0.500
Cathode-3	0.12	<0.500	<1.000	<0.500	<1.00	<1.0	<3.0	<0.500	<0.500
Test 2									
Cathode-1	<0.100	<0.500	<1.000	<0.500	<1.00	<1.0	<3.0	<0.500	<0.500
Cathode-2-W	<0.100	0.81	1.15	0.5	<1.00	1.1	<3.0	<0.500	<0.500
Cathode-2-E	<0.100	<0.500	<1.000	<0.500	<1.00	1.1	<3.0	<0.500	<0.500
Cathode-3	<0.100	<0.500	1.01	<0.500	<1.00	1.2	<3.0	<0.500	<0.500
Test 3									
Cathode-1	<0.100	<0.500	<1.000	<0.500	<1.00	<1.0	<3.0	<0.500	<0.500
Cathode-2-W	<0.100	<0.500	<1.000	<0.500	<1.00	<1.0	<3.0	<0.500	<0.500
Cathode-2-E	<0.100	<0.500	<1.000	<0.500	<1.00	<1.0	<3.0	<0.500	<0.500
Cathode-3	1.28	5.08	1.11	1.43	<1.00	1.1	3.6	<0.500	0.54
Test 4									
Cathode-1	<0.100	<0.500	1.03	<0.500	<1.00	1.2	<3.0	<0.500	<0.500
Cathode-2-W	<0.100	<0.500	1.24	<0.500	<1.00	1.1	<3.0	<0.500	<0.500
Cathode-2-E	<0.100	<0.500	1.19	<0.500	<1.00	1.1	<3.0	<0.500	<0.500
Cathode-3	<0.100	<0.500	1.32	<0.500	<1.00	1.2	<3.0	<0.500	<0.500
Test 5									
Cathode-1	<0.100	<0.500	1.06	0.5	<1.00	2.1	<3.0	<0.500	<0.500
Cathode-2-W	<0.100	<0.500	1.2	<0.500	<1.00	1.9	<3.0	<0.500	<0.500
Cathode-2-E	<0.100	<0.500	1	<0.500	<1.00	1.7	<3.0	<0.500	<0.500
Cathode-3	<0.100	<0.500	1.17	<0.500	<1.00	1.7	<3.0	<0.500	<0.500
Test 6									
Cathode-1	0.1	0.8	<1.000	<0.500	<1.00	<1.0	<3.0	<0.500	<0.500
Cathode-2-W	<0.100	0.79	<1.000	<0.500	<1.00	<1.0	<3.0	<0.500	<0.500
Cathode-2-E	0.11	0.98	<1.000	<0.500	<1.00	<1.0	<3.0	<0.500	<0.500
Cathode-3	0.1	0.84	<1.000	<0.500	<1.00	<1.0	<3.0	<0.500	<0.500
Test 7									
Cathode-1	<0.100	0.89	1.12	<0.500	<1.00	<1.0	<3.0	<0.500	<0.500
Cathode-2-W	<0.100	1.47	<1.000	<0.500	<1.00	<1.0	<3.0	<0.500	<0.500
Cathode-2-E	0.15	0.98	1.05	0.59	<1.00	<1.0	<3.0	<0.500	<0.500
Cathode-3	<0.100	0.76	<1.000	<0.500	<1.00	<1.0	<3.0	<0.500	<0.500

All units in ppm.

levels in the resulting cathode copper are similar as in Test-2. The effects of low flow rate on impurities levels in the harvested copper are further discussed in Section IV–D. Test-7 was performed under low cell temperature using the type-2 anodes and the wide cathode blanks. Nevertheless, the cell temperature could not be largely reduced and 330 K (57 °C) is the lowest temperature that can be reached because of the system design. From the results shown in Table V, the type-2 anodes performed well under slightly lower cell temperature as compared with Test-2, and low bismuth level cathode copper was produced.

The adhered slimes on the harvested anodes and the released slimes in the cell including settled and suspended slimes were collected after each test. A photo of the remaining anode with adhered slimes is shown in Figure 4. The weights of cell slimes and adhered slimes were measured for each test, which are shown in Table VI.

It can be observed that the adhered slime weight ratio is about 0.18 in the control test and it increases to 0.5 in Test-2 using the type-2 anodes. A similar weight ratio of

Fig. 4—The harvested anode with adhered anode slimes after the copper electrorefining experiment.

adhered slimes is observed in Test-3 using the type-3 anodes. In Test-4 that was conducted under high current density using the type-1 anodes, the total weight of slimes decreases significantly and the adhered slimes occupy almost three-fourths of all slimes in weight. In Test-5 where the wide cathode blanks were utilized, the weight of total slimes is also reduced, with most of the slimes as cell slimes. In Test-6 that was performed under low flow rate using the type-2 anodes, the total slime weight is not lowered and almost all slimes exist in the

Table VI. Weights and Weight Ratios of Cell Slimes and Adhered Slimes for Each Test

Test Number	Test-1	Test-2	Test-3	Test-4	Test-5	Test-6	Test-7
Cell slime weight (g)	392	356	222	32	183	882	816
Cell slime weight ratio (percent)	82.18	49.58	48.16	25.81	98.92	99.77	97.84
Adhered slime weight (g)	85	362	239	92	2	2	18
Adhered slime weight ratio (percent)	17.82	50.42	51.84	74.19	1.08	0.23	2.16
Total slime weight (g)	477	718	461	124	185	884	834

Fig. 5—The harvested anode with distinct surface morphologies after copper electrorefining Test-6.

form of cell slimes. The resulting anodes have interesting surface morphologies, which are shown in Figure 5. Similar phenomenon happened in Test-7 that was conducted under low cell temperature using the type-2 anodes, with a slightly higher weight ratio of adhered slimes. Consequently, the type-2 high impurity level anodes and the type-3 low impurity level anodes present better anode slime adhesion than the type-1 anodes with mid-level impurities contents; high current density condition lowers the total weight of slimes and improves adhesion of anode slimes; the wide cathode blanks with normal cathodic current density result in lowered total weight of slimes and very poor anode slime adhesion, probably due to the much higher current density on the anodes; the low flow rate test and the low cell temperature test also show poor slime adhesion on the anode with quite large amounts of cell slimes, which could be the results of the interaction between high impurities contents in the anodes and high current density on the anodes (due to the use of wide cathode blanks). These will be further discussed in Section IV. Nevertheless, the low cell temperature test (Test-7) will not be further discussed, because the temperature drop was not significant enough to observe or arrive at a conclusion on the effects of cell temperature on slime adhesion and transport in the pilot-scale electrorefining cell.

IV. DISCUSSION

A. *The Effect of Anode Compositions*

The effects of impurities contents in the anode on slime behavior and cathode purity can be discussed from the results of Test-2, Test-3, and the control test. In order to analyze the inclusion particle types in each type of anodes, the cross sections cut from the type-1, type-2, and type-3 anodes were polished and observed under SEM/EDS. The results are shown in Figures 6, 7, and 8, which include a SEM image, an EDS overlapping map including several elements' distributions, and four individual elemental distribution maps for significant elements.

From Figures 6, 7, and 8, it can be seen the inclusion particle types in these three types of anodes are similar. Firstly, lead, bismuth, sulfur, and arsenic have similar distributions in the anodes and are mostly distributed at the outer coating around inclusion particles, while oxygen has different distribution than other elements and is mostly distributed at the core of inclusion particles with copper. Therefore, oxygen plays the role of forming copper oxide cores (most likely to be cuprous oxide according to previous studies[6]), and lead, bismuth, sulfur, and arsenic generally constitute the outer shell of inclusions. Sometimes, cuprous selenide can also form the core as demonstrated in previous research.[2,6] Secondly, there are some cuprous oxide cores without coatings distributed in the anodes, due to insufficient amounts of lead, bismuth, sulfur, and arsenic.[2] Thirdly, Pb-Bi-S-As compound-isolated particles exist in the anodes. Consequently, most inclusion particles in the three different types of anodes have Cu-O cores with Pb-Bi-S-As shells and the remaining inclusions are uncoated Cu-O cores and Pb-Bi-S-As compound-isolated particles. The mechanism of forming Cu-O core with Pb-Bi-S-As shell inclusion particles is that[2] copper oxide generally has melting temperature around 1273.15 K (1000 °C) and would be solidified first in the grain boundary region; the Pb-Bi-S-As compounds have lower melting temperatures and would solidify around the preformed Cu-O cores.

However, the three types of anodes have some differences in terms of inclusion particles, according to Figures 6, 7, and 8. Firstly, cuprous oxide cores are better surrounded by Pb-Bi-S-As shells in the type-2 and type-3 anodes. Secondly, arsenic distribution in Pb-Bi-S-As compounds is almost as dense as the distributions of lead and bismuth in the type-1 anodes, but is not in the type-2 and type-3 anodes. These should be due to the high Pb/As ratio (about 2) in the type-2 and type-3 anodes and the low Pb/As ratio (about 1) in the type-1 anodes. According to previous study,[2] inclusion particles with Pb-Bi-S shells have lower sintering temperatures and are easier to adhere to the anode surface and coalesce as larger particles, than inclusion particles with

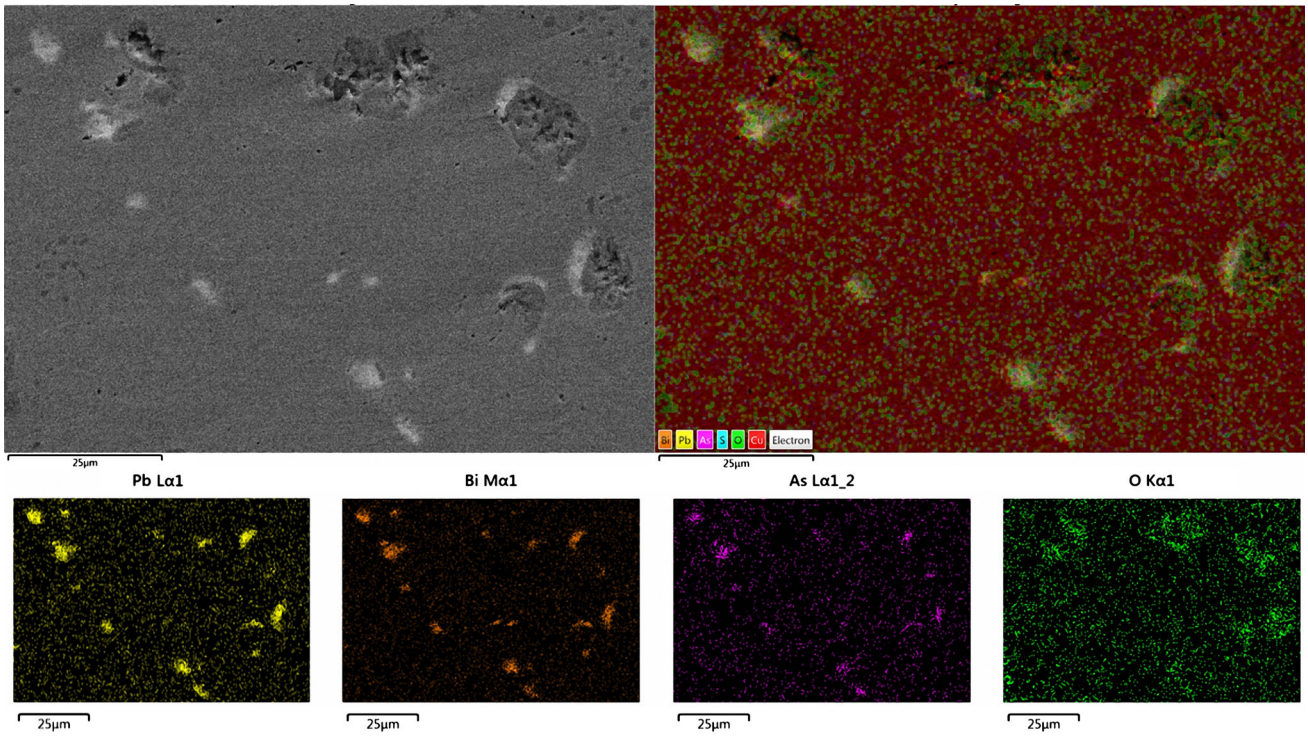

Fig. 6—SEM/EDS images of the cross section of the type-1 anodes used in the tests.

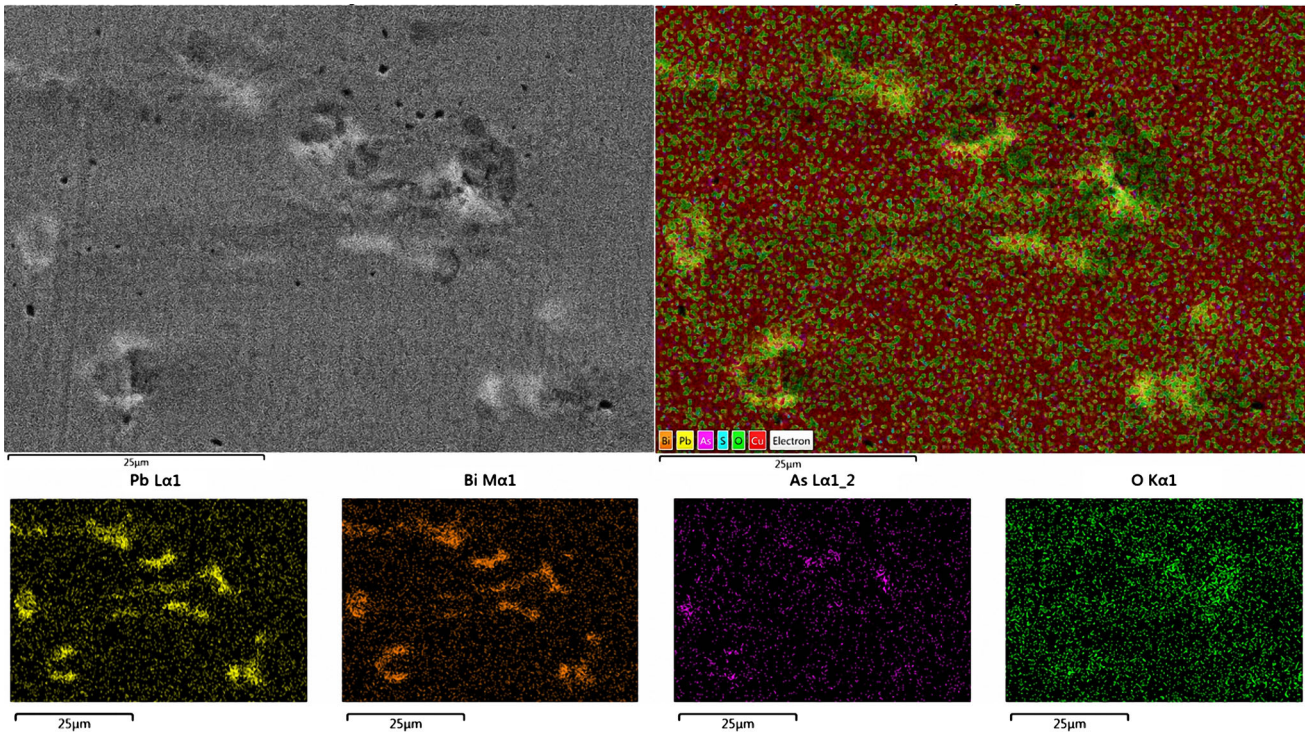

Fig. 7—SEM/EDS images of the cross section of the type-2 anodes used in the tests.

Pb-Bi-S-As shells. This is mostly because that the addition of high-melting temperature arsenic would increase the sintering temperatures of the shells. Although As-O core with Pb-Bi-S shell inclusion particles are not formed in the three types of anodes, the relative content of arsenic in Pb-Bi-S-As shells of existing inclusion particles should affect their sintering and coalescence temperatures. In order to examine arsenic distribution in Pb-Bi-S-As shells of the inclusions in the three different types of anodes, EDS area

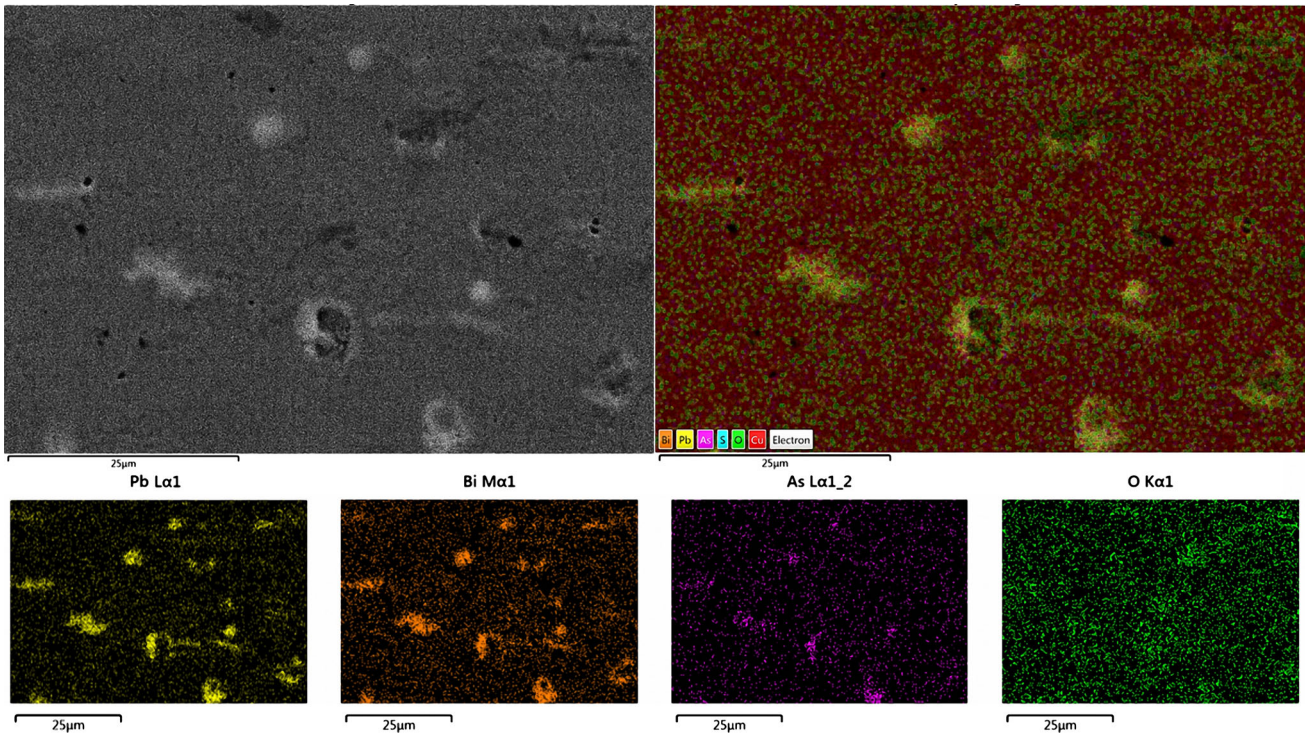

Fig. 8—SEM/EDS images of the cross section of the type-3 anodes used in the tests.

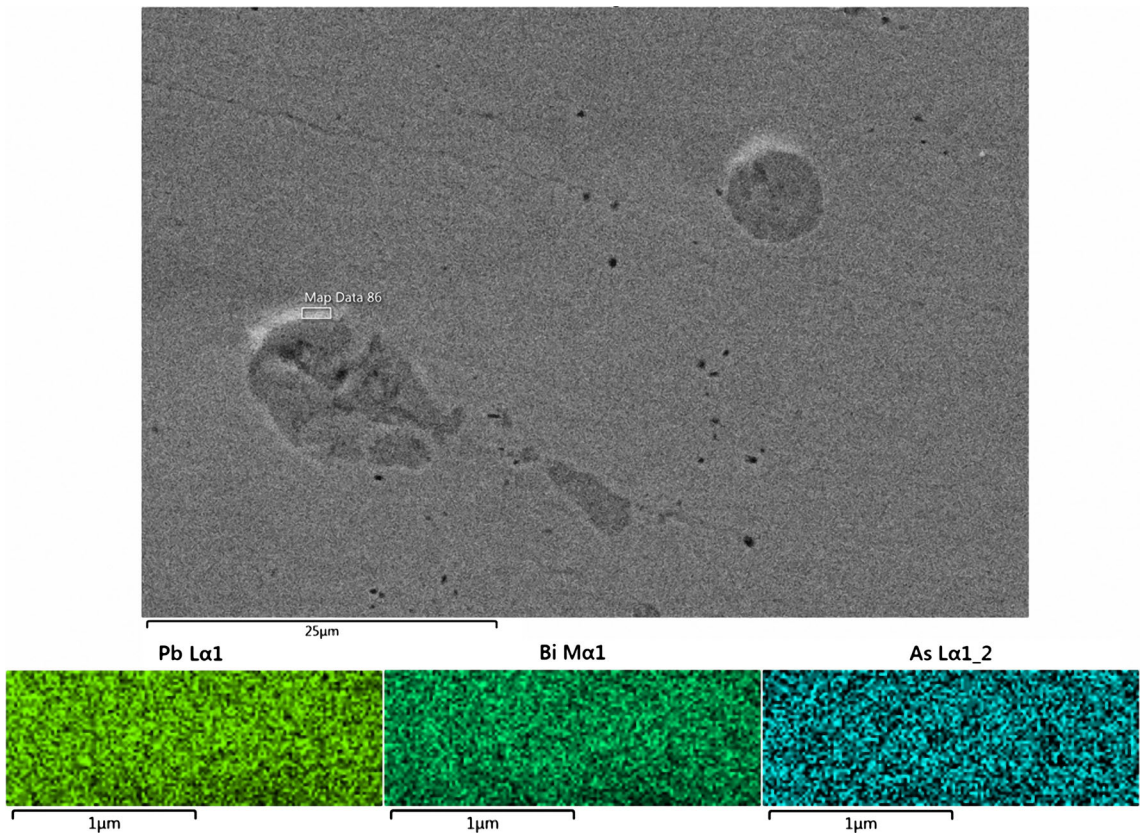

Fig. 9—EDS area scan on the shell of a typical inclusion particle in the type-1 anodes.

scans on inclusion particle shells were performed. Typical arsenic distribution in the shell of inclusions in the type-1 anodes is shown in Figure 9. The type-2 and type-3 anodes have similar arsenic distribution in the shell of their inclusion particles, which is shown in Figure 10.

It can be seen that the relative arsenic content in comparison with lead and bismuth in the shell of inclusion particles is much higher in the type-1 anodes than in the type-2/type-3 anodes. This is very likely due to the lower Pb/As ratio in the type-1 anodes compared with the type-2 and type-3 anodes. Since the sintering and coalescence of slime (inclusion) particles are mostly affected by their shells, the slime particles from the type-2 and type-3 anodes can coalesce together and adhere to the anode more easily than those from the type-1 anodes, because of lower sintering temperatures due to lower arsenic content in the shell and more coatings (shell) on the core (as shown in Figures 6, 7, and 8). Consequently, Test-2 and Test-3 have better anode slime adhesion (as shown in Table VI) and less bismuth levels in the harvested cathode copper (as shown in Table V) except Cathode-3 in Test-3. This cathode was slightly tilted to Anode-2 during the test due to uneven sitting surface and could have more slime particles deposited. The effects of the relative arsenic content in the shells of slime particles can be further discussed with the ICP results of the compositions of the slimes collected from the tests, which are shown in Table VII.

As shown in Table VII, the adhered anode slimes have a higher Pb/As ratio than the cell slimes (released slimes) in both tests, which indicates that slime particles with a higher lead-to-arsenic ratio in their shells (cores are mostly Cu_2O) can sinter together and adhere to the anode more easily than those with a lower lead-to-arsenic ratio in the shells.

In sum, anodes with a lead-to-arsenic ratio larger than 1.5 perform better in copper electrorefining by having larger amount of adhered slimes and producing cathode copper with lower bismuth levels, than anodes with almost equal amounts of lead and arsenic. Anodes with

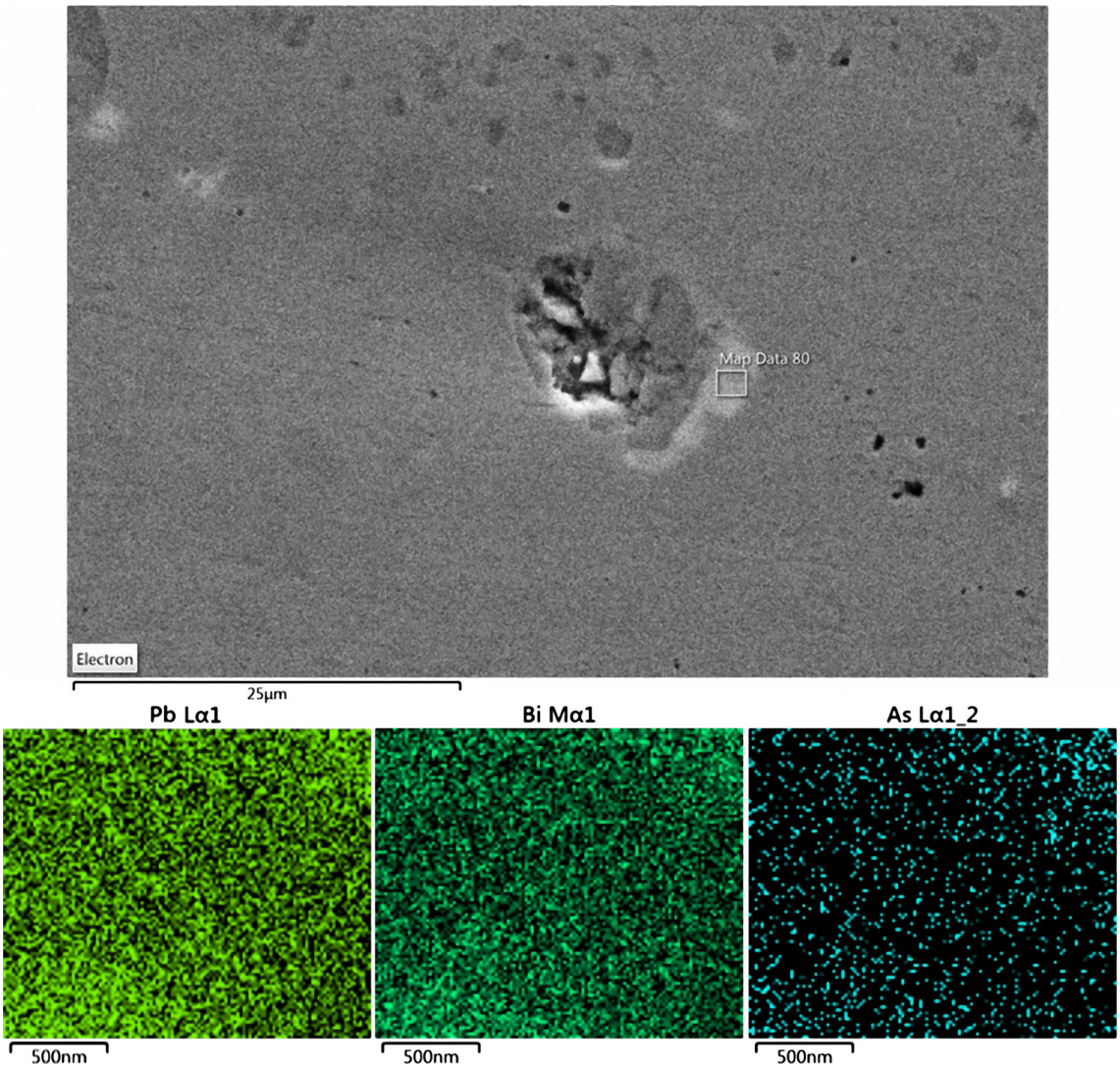

Fig. 10—EDS area scan on the shell of a typical inclusion particle in the type-2/type-3 anodes.

Table VII. Compositions of Different Types of Slimes Collected from Test-1 and Test-2

Test Number	Slime Type	Pb	As	Bi	Cu	Se	Te	Sb	Sn	Pb/As
Test-1	adhered slime	23.5	4.94	4.43	25.8	7.64	0.959	0.3	0.033	4.8
	cell slime	15.11	3.94	3.01	19.6	4.43	0.602	0.316	0.05	3.8
Test-2	adhered slime	34	2.95	3.64	15	2.65	0.934	0.423	0.068	11.5
	cell slime	21.7	2.08	2.28	8.65	2.03	0.48	0.289	0.031	10.4

All units in weight percent.

Table VIII. Compositions of Different Types of Slimes Collected from Test-4 and the Control Test

Test Number	Slime Type	Pb	As	Bi	Cu	Se	Te	Sb	Sn	Pb/As
Test-4	adhered slime	23.59	4.08	5.85	<0.0004	7.38	1.17	0.386	0.045	5.8
	cell slime	18.35	4.02	4.79	22.3	4.95	0.81	0.344	0.042	4.6
Test-1	adhered slime	23.5	4.94	4.43	25.8	7.64	0.959	0.3	0.033	4.8
	cell slime	15.11	3.94	3.01	19.6	4.43	0.602	0.316	0.05	3.8

All units in weight percent.

a lead-to-arsenic ratio smaller than one are not studied in these tests, but according to previous study,[2] they produced high-purity cathode copper by forming inclusion particles with As-O cores and Pb-Bi-S shells.

B. *The Effect of High Current Density*

From the results of Test-4 using the type-1 anodes under an average cathodic current density of 300 A/m^2, the effects of high current density on the behavior of slime particles and the production of cathode copper can be discussed by comparison with the control test. The most significant findings in Test-4 include (1) the anode slime adhesion is exceptionally good (74.19 pct adhered slimes, compared with 17.82 pct in the control test); (2) the total weight of slimes collected in Test-4 is reduced by 74 pct from that in the control test; (3) the bismuth levels in the cathode copper are reduced to lower than 0.1 ppm, which is better than the copper produced in the control test. Apparently, the anode slimes have significantly different behavior in this test and therefore the compositions of different types of slimes collected in the test need to be analyzed in order to find the reasons for these phenomena. The results are shown in Table VIII.

It is very interesting that the copper concentration in the adhered slimes is less than 0.0004 wt pct, which means almost no copper is left in the attached slimes after this high current density copper electrorefining test. Note that under high current density, the heat generated on the anodes by contact resistance is larger than that under normal conditions and the local temperatures at the anode surface would be higher than those in Test-1. The temperatures of the electrolyte in the inter-electrode gap in Test-4 and the control test were measured by using an infrared thermometer. The electrolyte temperature in the gap increased about 3 K from around 335 K (62 °C) in the control test to about 338 K (65 °C) in Test-4. Additionally, the number of slime particles released from the copper matrix per unit time is larger compared with Test-1. As a result, more sintering and coalescence of slime particles can take place in front of the anode surface, leading to better adhesion of slimes on the anode. When the larger current passes through the stronger adhered anode slimes on the remaining copper anode, the cuprous oxide core and even part of the shell of slime particles can be dissolved by this current. The dissolution of part of slime particles results in lighter weight of anode slimes layer. Therefore, even under same adhesion strength, more slime particles can be kept in the layer. Slime particles that have a smaller lead-to-arsenic ratio would fall off the anodes as discussed in Section IV–A, and the cuprous oxide cores would be kept in the slimes. These explain the different compositions of the two types of slimes from Test-4. Besides, the collected cell slimes and adhered slimes were observed under SEM/EDS, which are shown in Figures 11 and 12. Note that structures of slime particles might be affected in the process of collection. Some charging issues are reflected on the images of Figure 12, due to the poor electrical conductivity of slime particles.

From Figure 11, it can be observed that the cell slimes collected in Test-4 show the existence of a large amount of element copper, which indicates that most cuprous oxide cores remain in the released slimes from the anode. From Figure 12, it can be observed that the adhered slimes on the anode do not have much copper left but have significant amounts of lead, bismuth, arsenic. Many shell-like structures agglomerated together and can be seen in the SEM image of the adhered slimes, which means that most cuprous oxide cores have been consumed by the large current passing through the anode slimes layer. Another SEM image of the adhered slimes from Test-4 is shown in Figure 13 and it can be seen that these slime particles have almost only shells left with most of their cuprous oxide cores consumed. The dissolutions of cuprous oxide cores and even part of shells lead to the weight loss of slime particles collected in Test-4.

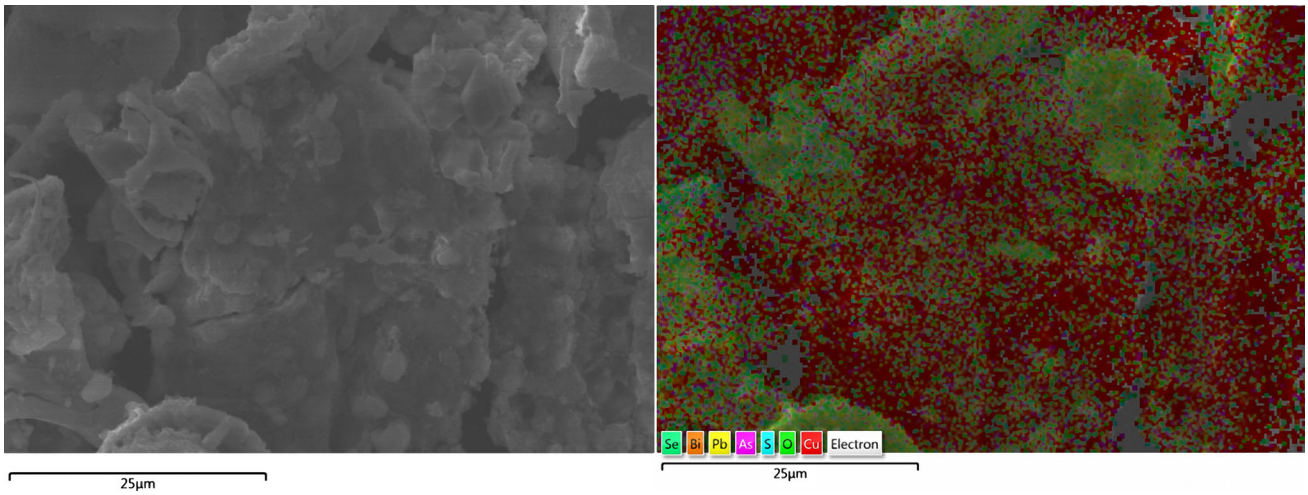

Fig. 11—SEM image and EDS layered map of elemental distributions for cell slimes collected in Test-4.

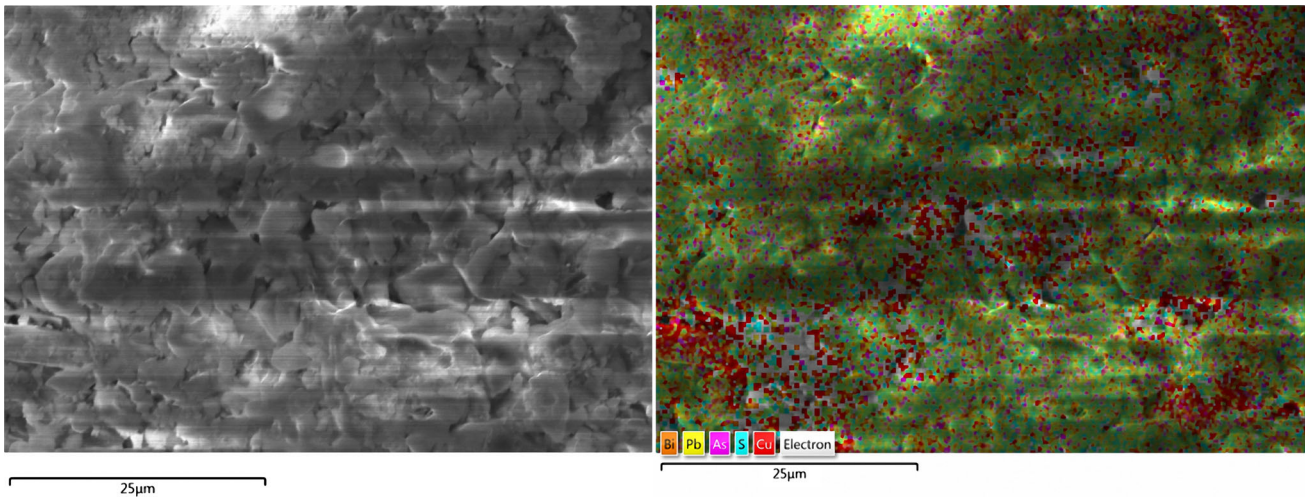

Fig. 12—SEM image and EDS layered map of elemental distributions for adhered slimes stripped from the residual anodes in Test-4.

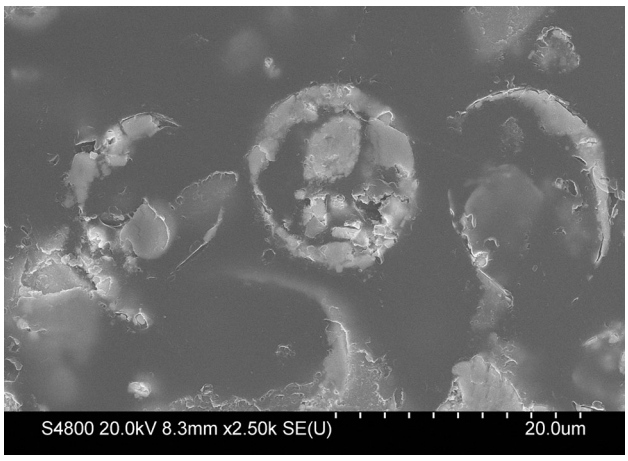

Fig. 13—SEM image of the adhered slimes stripped from the residual anodes in Test-4.

The better control of bismuth levels in the harvested copper in Test-4 mostly results from the largely improved anode slime adhesion with less slimes released to the electrolyte. In addition, higher current densities on the anodes can create larger electrolyte density gradients along the anodes, which can result in downward electrolyte flows with larger magnitudes.[4] Then the released slimes have greater opportunities to settle to the cell bottom rather than to stay in the electrolyte flow and get entrapped in the cathode copper.

Consequently, high current density condition can be a solution for copper electrorefining using anodes with a lead-to-arsenic ratio of approximately one. High current density can lead to more sintering and coalescence of slime particles and lighter weight of anode slimes layer, which give better anode slime adhesion. Also, it generates faster downward electrolyte flows along the anodes, which help settle the released slimes to the bottom of the cell.

C. *The Effect of Wide Cathode Blanks*

From the results of Test-5, the wide cathode blanks generally have two major effects in the process. Firstly, since the wide blanks are approximately 1.36 times as large as the normal blanks in width and deposition area, the anodic current density under the condition of 240 A/m^2 cathodic current density on the wide blanks is even higher than that under the condition of 300 A/m^2 cathodic current density on the normal blanks. The total current on the anodes is 81 A in Test-4 and 98 A in Test-5, with the same anode dimensions throughout all the tests. Secondly, wider cathode blanks provide more chances to entrap slime particles moving in the gap between each adjacent anode and cathode. Therefore, there could be some impurity concentration differences between the edges and the center of cathode copper, which will be discussed in this section.

The compositions of the two types of slimes collected in Test-5 were also analyzed by ICP and the results are shown in Table IX.

Notice that the weight of adhered slimes in Test-5 is only 2 g and most slimes are cell slimes that are 183 g. Under the condition of even higher anodic current density, the copper in the slime particles in Test-5 were not consumed as dramatically as Test-4. Also, the anode slime adhesion is very poor in Test-5, as the weight percentage of adhered slimes is only 1.08 pct. These indicate that the adhered slimes failed to keep attached on the anode surface for the cuprous oxide cores to be completely dissolved. Rather, they fell off the anode after partial dissolution of cores, with about 14 pct of copper left. The dissolution of the shells of slime particles may become more intense under this high anodic current density. The reason behind this phenomenon could be that the sintering and coalescence of slime particles in front of the anode become so intensive under such high anodic current density that the adhesion force cannot hold the resulting large slime particle aggregates anymore. Besides, the number of anode slimes released from copper matrix per unit time is even larger than Test-4 and thus the sizes of anode slime aggregates can increase very quickly with the fast release of slime particles. Consequently, most anode slimes would fall off the anode due to their large sizes before the complete dissolution of cuprous oxide cores. The fact that the impurities levels in the harvested copper were well controlled in Test-5 may demonstrate that the sizes of most cell (released) slimes in Test-5 are sufficiently large to settle down with less opportunities to affecting the purity of cathode copper. After all, suspended slimes are the major source of cathode contamination rather than settled slimes.[2]

To examine the edge effect of wide cathode blanks, the edges of the harvested copper from cathode-1 and cathode-2-W were cut off and analyzed separately for impurities concentrations, in order to compare with those in the center. The results are shown in Table X. Note that the width of the cut edges is equivalent to the width difference between the normal blank and the wide blank. So we can determine whether the extra areas on the wide blanks are more contaminated or not. Also notice that these edge and center samples were cut at the same height on the cathode.

In Table X, Cathode-1-L, Cathode-1-C, and Cathode-1-R represent the left edge, the center, and the right edge of Cathode-1, respectively. The same naming method applies for Cathode-2-W. It can be observed from the results that the edges of the harvested copper contain more impurities than the centers of the cathode copper. For example, the left edge of Cathode-1 has too high contents of bismuth, arsenic, and lead, and thus could not be further processed if produced in real plants. In contrast, the centers of Cathode-1 and Cathode-2-W have low levels of impurities and are acceptable for

Table IX. Compositions of Different Types of Slimes Collected from Test-5 and the Control Test

Test Number	Slime Type	Pb	As	Bi	Cu	Se	Te	Sb	Sn	Pb/As
Test-5	adhered slime	24.39	1.16	2.44	10.5	6.92	0.8	0.151	0.053	21.0
	cell slime	30.28	3.11	3.22	13.6	4.35	0.759	0.295	0.054	9.7
Test-1	adhered slime	23.5	4.94	4.43	25.8	7.64	0.959	0.3	0.033	4.8
	cell slime	15.11	3.94	3.01	19.6	4.43	0.602	0.316	0.05	3.8

All units in weight percent.

Table X. Impurities Concentrations in the Edges and Centers of the Harvested Copper from Cathode-1 and Cathode-2-W in Test-5

Impurity	Bi	As	Pb	Se	Sb	Ni	Fe	Sn	Te
Test 5									
Cathode-1-L	0.8	4.16	5.53	<0.500	<1.00	2.2	3.3	<0.500	0.54
Cathode-1-C	0.12	1.68	0.73	<0.500	<1.00	<1.0	3.6	<0.500	<0.500
Cathode-1-R	0.13	3.89	0.76	<0.500	<1.00	1.3	3.7	<0.500	<0.500
Cathode-2-W-L	0.38	2.76	2.15	<0.500	<1.00	1.8	5.9	<0.500	<0.500
Cathode-2-W-C	0.1	<1.000	0.5	<0.500	<1.00	<1.0	3.2	<0.500	<0.500
Cathode-2-W-R	0.11	2.18	<0.500	<0.500	<1.00	1.4	<3.0	<0.500	<0.500

All units in ppm.

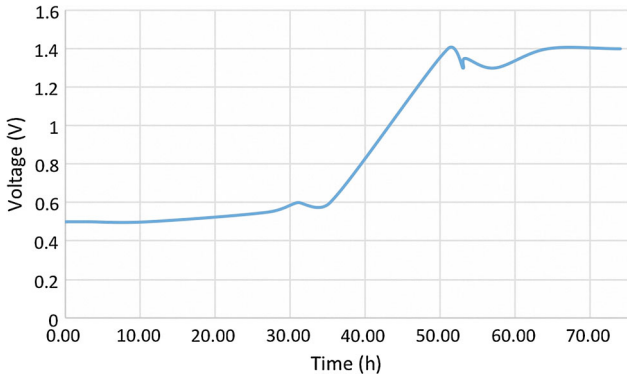

Fig. 14—Cell voltage *vs* time at the beginning of the passivation during Test-6.

further processing. Therefore, the results indicate that cathode blanks that are wider than the anode (4.75 inches (0.12 m) *vs* 4.2 inches (0.11 m)) can entrap more slime particles due to the edge effect. Thus the cathode width to anode width ratio is better to be less than one in order to have purer cathode copper. However, the current distribution and production rate would be affected if the cathode blank is narrow than the anode. A better method is to cut off the edges of sub-quality cathodes whose impurity levels are beyond the limits, in order to make the rest of the cathodes meet the purity requirements.

In total, the wide cathode blanks intensify the sintering and coalescence of slime particles in front of the anode by raising the anodic current densities. When the sizes of the large slime aggregates increase to a certain point where they cannot be supported by the adhesion force anymore, the slime aggregates would fall off the anode and settle to the cell bottom. Therefore, the cathode copper in Test-5 was not much influenced by the released slimes though the anode slime adhesion was poor under such conditions. Furthermore, edge effects of the wide cathode blanks were found by analyzing the impurities contents in the edges and the centers of the harvested copper. The results show that the edges have higher impurities levels than the centers.

D. *The Effect of Low Flow Rate*

Test-6 was performed under the flow rate of 2.5 mL/second, which is half of the normal value. The anodes used are the type-2 anodes, which have slime particles with lower sintering temperatures than those from the type-1 anodes as discussed in Section IV–A. The wide cathode blanks were utilized in the test. Note that the electrolyte temperature in the four electrode gaps dropped about 4 K from the normal value of 334 K (61 °C) due to less heat convection from the inlet flow and the temperature was 334 K (61 °C) in regions near the inlet. Passivation was observed on the surfaces of the anodes especially in Anode-2 during Test-6, and the voltage changes as the passivation began are shown in Figure 14. Distinct surface morphologies were observed on the anodes after passivation, as shown in Figure 5.

The occurrence of passivation is usually accompanied by the formation of copper oxide layers attached to the anode, and the poor heat and electrical conductivities of the layers can elevate local temperatures in front of the anode.[2] Thus the local temperatures could be raised back though the cell temperature dropped. Furthermore, the type-2 anodes have slime particles that are easier to sinter together (high Pb/As ratio) and coalesce as larger particles than the type-1 anodes under similar temperatures. As a result, with the same anodic current density, slime particles in front of the anode in Test-6 can have more intensive sintering and coalescence than Test-5, which can lead to very early release of larger slime particle aggregates from the anode before the consumption of cuprous oxide cores. The compositions of the slimes collected in Test-6 confirm the early release of cell slimes before the cores can dissolve under the high anodic current density. The results are shown in Table XI.

The results of Test-2 are shown in Table XI instead of the control test, because the type-2 anodes were used in both Test-6 and Test-2. Note that the adhered slimes are only 2 g in this test and the remaining adhered slimes were dissolved significantly by the high current according to Table XI. Copper in the cell slimes were almost not consumed, which means that most slimes did form large slime aggregates and fall off the anode surface very early due to the very intense sintering and coalescence of the slime particles. The inlet electrolyte flow had smaller velocities in Test-6 due to the low flow rate and thus generated less agitation at the bottom of electrodes. Consequently, the released large slimes could settle down more easily and had less effects on cathode copper, which is consistent with the low levels of bismuth in the harvested copper from Test-6.

Therefore, low flow rate exerts effects on anode slime behavior in front of the anode. Although it results in temperature drop in the bulk solution, low flow rate increases local temperatures in front of the anode by causing anode passivation and forming oxide layers. With the type-2 anodes and wide cathode blanks under such conditions, slimes can coalesce as large particles and fall off quite early due to very intense slime particle

Table XI. Compositions of Different Types of Slimes Collected from Test-6 and Test-2

Test Number	Slime Type	Pb	As	Bi	Cu	Se	Te	Sb	Sn	Pb/As
Test-6	adhered slime	13.36	0.691	0.722	7.58	1.34	0.288	0.098	0.032	19.3
	cell slime	17.4	2.32	1.26	15.3	2.62	0.576	0.161	0.026	7.5
Test-2	adhered slime	34	2.95	3.64	15	2.65	0.934	0.423	0.068	11.5
	cell slime	21.7	2.08	2.28	8.65	2.03	0.48	0.289	0.031	10.4

All units in weight percent.

Table XII. Optimal Anode Composition and Operating Conditions for Copper Electrorefining Based on the Results of This Study

Parameters	Pb/As Ratio	Cathode Current Density	Flow Rate/Velocity/Residence Time	Cathode Size
Optimal value/range	>1.5	300 A/m^2 with normal blank 240 A/m^2 with wide blank	5 mL/s 0.04 m/s 3.3 hours residence time	normal blank for high quality wide blank for high productivity

sintering and coalescence, without significant dissolution of cuprous oxide cores. Low flow rate can also reduce the agitation below the electrodes and thus help these large slime particles settle even faster.

V. CONCLUSIONS

A series of copper electrorefining tests were performed in a pilot-scale cell to examine the effects of anode compositions, current density, cathode blank width, temperature, and flow rate on the anode slime behavior and cathode copper purity. Although the effect of temperature could not be determined due to limited temperature changes that can be reached in the cell, other factors demonstrated significant effects on slime adhesion and cathode purity. Since the experiments were conducted using the same electrolyte as the commercial cells in a large electrorefining cell under tankhouse environment, the results and analyses are valuable for directing industrial copper electrorefining process. Table XII suggests a set of optimal operating conditions for copper electrorefining based on the results of this study.

First of all, the anode compositions, especially the contents of lead and arsenic, affect the anode slime behavior. Anodes that have a lead-to-arsenic ratio larger than 1.5 demonstrated better anode slime adhesion and lower impurity levels in cathode copper than the anodes that have similar amounts of lead and arsenic. This is mostly because that the relative arsenic content in the shell of inclusion particles can affect their sintering temperatures. Inclusion particles in the anodes with the lead-to-arsenic ratio larger than 1.5 have less arsenic content in the shell and thus have lower sintering temperatures. Therefore, these particles are easier to coalesce together and adhere to the anode, with less opportunities to fall off and/or reach the cathode.

Secondly, high current density can intensify the sintering and coalescence of slime particles. Besides, it can heavily dissolve the cuprous oxide core in slime particles, leading to lighter weight of anode slimes layer. Thus the anode slime adhesion is improved under high current density, with larger percentages of adhered slimes on the anode. It can help reducing impurities levels in copper electrorefining using anodes with the lead-to-arsenic ratio close to one.

Thirdly, wide cathode blanks with the same cathodic current density can significantly intensify slime particles' sintering and coalescence in front of the anode by largely increasing the anodic current density. Under such conditions, the slime particle aggregates would grow to a point where the adhesion force cannot support their weights anymore. As a result, the slime particle aggregates would fall off the anode and settle down due to their too large sizes. Therefore, the produced cathode copper have low impurities levels, though the amount of cell (released) slimes is considerably large under these conditions. In addition, the edges of cathode copper were shown to be more contaminated than the center.

Lastly, low flow rate generally causes less agitation under the electrodes, lower bulk electrolyte temperature and anode passivation that can raise local temperatures in front of the oxide layers attached to the anode. When anodes with the lead-to-arsenic ratio larger than 1.5 and wide cathode blanks were used under such conditions, the sintering and coalescence of slime particles in front of the anode would be very intense and the slime particles would fall off the anode quite early without significant dissolution of cores.

REFERENCES

1. M.L. Free: *Hydrometallurgy: Fundamentals and Applications*, Wiley, Hoboken, 2013, pp. 229–32.
2. W. Zeng, M.L. Free, and S. Wang: *J. Electrochem. Soc.*, 2016, vol. 163, pp. E14–31.
3. W. Zeng, J. Werner, and M.L. Free: *Hydrometallurgy*, 2015, vol. 156, pp. 232–38.
4. W. Zeng, M.L. Free, J. Werner, and S. Wang: *J. Electrochem. Soc.*, 2015, vol. 162, pp. E338–52.
5. W. Zeng, S. Wang, and M.L. Free: *J. Electrochem. Soc.*, 2016, vol. 163, pp. E111–22.
6. T.T. Chen and J.E. Dutrizac: *JOM*, 1990, vol. 42, pp. 39–44.
7. T.T. Chen and J.E. Dutrizac: *Can. Metall. Q.*, 1988, vol. 27, pp. 91–96.
8. T.T. Chen and J.E. Dutrizac: *Can. Metall. Q.*, 1990, vol. 29, pp. 27–37.
9. T.T. Chen and J.E. Dutrizac: *Can. Metall. Q.*, 1989, vol. 28, pp. 127–34.
10. T.T. Chen and J.E. Dutrizac: *Can. Metall. Q.*, 1991, vol. 30, pp. 95–106.
11. T.T. Chen and J.E. Dutrizac: *Metall. Mater. Trans. B*, 2005, vol. 36B, pp. 229–40.
12. T.T. Chen and J.E. Dutrizac: *Can. Metall. Q.*, 1988, vol. 27, pp. 97–105.
13. J.D. Scott: *Metall. Trans. B*, 1990, vol. 21B, pp. 629–35.
14. T.T. Chen and J.E. Dutrizac: *Metall. Trans. B*, 1989, vol. 20B, pp. 345–61.
15. X. Cheng and J.B. Hiskey: *Metall. Mater. Trans. B*, 1996, vol. 27B, pp. 610–16.
16. J.B. Hiskey: *T.T. Chen Honorary Symposium on Hydrometallurgy, Electrometallurgy and Materials Characterization*, TMS, Wiley, Hoboken, 2012, pp. 101–12.
17. X. Wang, Q. Chen, Z. Yin, M. Wang, B. Xiao, and F. Zhang: *Hydrometallurgy*, 2011, vol. 105, pp. 355–58.
18. F.X. Xiao, Y.J. Zheng, Y. Wang, W. Xu, C.H. Li, and H.S. Jian: *Trans. Nonferrous Met. Soc. China*, 2007, vol. 15, pp. 1069–74.
19. S. Wang, D. Kim, and M. Moats: *Proc. Copp.*, 2013, vol. 5, pp. 577–94.
20. M. Moats, S. Wang, and D. Kim: *T.T. Chen Honorary Symposium on Hydrometallurgy, Electrometallurgy and Materials Characterization*, TMS, Wiley, Hoboken, 2012, pp. 3–21.
21. C.A. Moller and B. Friedrich: *Proc. Copp.*, 2010, vol. 4, pp. 1495–510.
22. J.E. Hoffmann: *JOM*, 2004, vol. 56, pp. 30–33.
23. S. Wang: *JOM*, 2004, vol. 56, pp. 34–37.
24. M.L. Free: *Hydrometallurgy: Fundamentals and Applications*, Wiley, Hoboken, 2013, pp. 218–28.